Dissertation Summary

Time resolved chromatin architecture and transcription regulation during the yeast respiratory cycle

Cornelia Amariei

Keio University
Institute for Advanced Biosciences
Graduate School of Media and Governance

This dissertation is presented for the fulfillment of the requirements for the degree of Doctor of Philosophy

September 2014

Abstract

Cellular rhythms, spanning from fast metabolic oscillators to circadian rhythms, are pervasive in many organisms. Their orchestration, crucial for the maintenance of cellular coherence, is poorly characterized due to difficulties in obtaining high-density time-series data where the cellular state is precisely defined. A system that overcomes these limitations is the continuous culture of *Saccharomyces cerevisiae*, in which cells auto-synchronize to produce respiratory oscillations that alternate between reductive and oxidative cellular states. This system has been used to investigate the interplay between the redox/energetic state and transcription, metabolite production and DNA replication, which revealed that the oscillation revolves around an alternation of anabolic and catabolic transcriptional programs leading to anabolic and catabolic phenotypes. This thesis investigates the role of chromatin architecture and its dynamics in the regulation of the transcriptional program. Previous datasets were analyzed with new computational tools developed for characterizing periodicities in high-throughput data, and the results pointed to an energy-dependent transcription regulation mechanism mediated by chromatin structure. Through CE-MS analyses of adenylate nucleotides, ChIP-qPCR and tiling array analyses of DNA occupancy, this study shows the existence of a global transcriptional reset point between the catabolic and anabolic transcriptional programs, characterized by a global nucleosome focusing event. The highly dynamic DNA occupancy correlates with changes in energy availability rather than transcriptional timing, suggesting that the initiation of anabolic and catabolic genes stems from differential effects of global remodeling events at gene promoters. An analysis of promoter regions revealed that a majority of genes are in close proximity, and many properties of gene transcription, i.e., average expression, noise, nucleosome occupancy, co-expression, correlate with the intergenic distance. These results point to global mechanisms underlying transcription regulation in eukaryotes, where the energetic state regulates global chromatin structure, and differential transcriptional outcomes stem from subtle differences in the promoter architecture.

Keywords: Yeast respiratory cycle • Transcription regulation • Redox oscillation • Chromatin dynamics • Time-series computational analysis

Chapter 1 Introduction

Rhythmicity within an organism spans a wide range of temporal scales, from fast neural rhythms (~10 ms)[1] to century-long flowering cycles[2]. Due partially to convenience and technical limitations, biological rhythms occurring on different time-scales have often been studied as separate phenomena, despite evidence that many processes show a temporal coordination[3–6]. In particular, studies on the interplay between circadian rhythms, cell cycle and metabolic rhythms have pointed to a coupling of these processes that seem to revolve around the cellular energetics and redox state[6–9], and involved transcriptional, translational and post-translational oscillators[10–12]. The medical implications are exemplified by the numerous links found between desynchronization or decoupling of these rhythms (e.g., heart rate, respiratory activity, hormone production, sleep cycle) and a variety of pathologies, such as mood disorders[13,14], obesity[15], breast cancer[16] and Parkinson's[17].

Between the frequencies of the most studied time domains, the circadian and the metabolic rhythms, lie the majority of cellular functions, such as metabolic transformations, transcription, translation, assembly of membranes and organelles, as well as the organization of chromosomal dynamics and the cell division cycles (typically in the minute and hour domains)[18]. Global rhythms have been shown in all these highly conserved processes in lower eukaryotes[19–23], some shown to be endogenous[24], or to occur in single mammalian cells[6]. In most studies however, the underlying rhythms remain masked by the lack of frequent time-series measurements necessary. Even when high temporal resolution is achieved, in a sample derived from a cell population, rhythms present in single cells can be hard to detect due to the asynchrony of the population, where time-averaging of processes and events that occur in out-of-phase individuals blur the dynamics of single cell organization. Therefore, the study of such dynamic processes requires either single-cell analyses or synchronized cell populations. While the former is greatly limited by the available technology and by difficulties in measuring an individual cell without irreversibly damaging it[25], the latter poses issues in the preparation of material without perturbation[26].

A convenient system that surpasses these challenges is exemplified by continuously-grown cultures of *S. cerevisiae*, which can become

spontaneously self-synchronized with respect to the cellular respiratory activity when grown at high density[27]. The period of the respiratory oscillation, characterized by alternation between oxidative and reductive phases, can range from 35 minutes to over a day depending on culture conditions[27–31]. Easy to monitor, to sample at high frequencies and without perturbation, this system has been reliable tool for acquiring time-series experimental data on the redox and energetic state[21,32], and various aspects of cellular life, e.g., metabolism[23,30], transcription[20,33,34], cell cycle[20], mitochondrial structure and organelle remodeling[23].

The respiratory oscillation in yeast is temperature-compensated[35] and its timekeeping characteristics define it as an ultradian clock. Moreover, several other properties of the respiratory oscillation are shared with the circadian clock, e.g., cell cycle gating[20,36], cellular energetics[31,37], redox biology[4], system-wide oscillations in mRNA[34,38] and metabolite abundances[21,39,40]. A recent study identified a redox-sensing clock in all domains of life[9], where the oxidation cycles of peroxiredoxins show clock characteristics and are coupled with circadian rhythmicity. These findings demonstrate a mechanism through which redox rhythmicity underlying cellular physiology could prove to be the rule rather than the exception across species[41]. In this context, the study of the respiratory ultradian rhythm in yeast continuous cultures, which involves alternation of redox states, can have a great impact on studies of higher organisms, where such analyses are more difficult to perform.

Chapter 2 The transcriptional program during the yeast respiratory cycle

A similar analysis was used to investigate the phase-relationship between transcription, energy availability and redox state (Fig. 1). The transcript abundance (Fig. 1A) for the anabolic, catabolic and noisy gene superclusters from time-series transcriptome dataset[34] were used to calculate the rate of change, as a proxy measure for transcriptional activity (Fig. 1B), revealing both the transcription initiation points (when rate of change becomes positive) for the anabolic (~280°) and catabolic (~50°) superclusters, and global patterns, such as an increase in transcript rate in mid-reductive phase (~220°) followed by a sharp drop before anabolic transcription. CE-MS time-series measurements showed oscillations of ATP which temporally coincide with global increases in

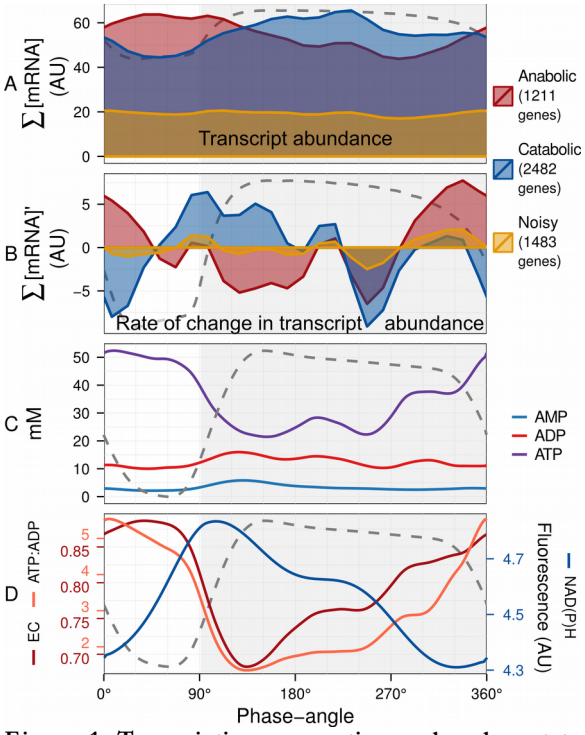

Figure 1 Transcription, energetics and redox state during an average respiratory cycle

Total mRNA abundances[34] for the gene expression super-clusters[31] (A; ∑[mRNA]) were used to calculate mRNA abundance rate of change (B; ∑[mRNA]'), as the change in mRNA abundance every 15°. Red shades indicate anabolic, blue shades indicate catabolic, and yellow shades indicate noisy genes. AMP, ADP & ATP concentrations (C) measured by CE-MS were used to calculate the energy charge (EC, D, red) and ATP:ADP (D, orange). NAD(P)H (D, blue) was measured by *in situ* fluorimetry[32]. An average cycle was constructed by a cubic spline fitting. Dotted lines represent the DO, scaled to the y-axis range of each panel, and datasets were aligned using the minimum and maximum first derivative of DO. The minimum first derivative of DO represents 0°/360°.

transcription rates (Fig. 1B,C). ATP:ADP (as a measure of ATP availability; Fig. 1D, red) and the adenylate energy charge, which spans the entire range reported for yeast[42] (EC; Fig. 1D, orange), peak in the oxidative phase and their recovery coincides with the transcription initiation in the anabolic supercluster. NAD(P)H (Fig. 1D, blue), as a proxy for cellular redox state, also shows a phase relationship with respiration and coincides with catabolic transcription initiation.

This high variability of energetic and redox potential during the yeast respiratory cycle emphasizes the diversity of naturally occurring physiological states. The phase relationships with the transcriptional activity, where maximal transcript turnover of anabolic and catabolic genes corresponds to the phases of transition between low and high energy states, implies an

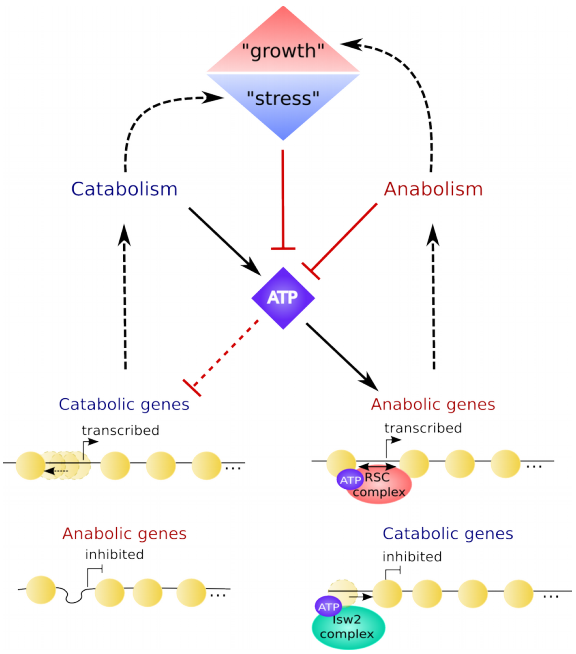

Figure 2 A dual negative feedback model depicting the direct influence of ATP on gene expression
High intracellular ATP availability leads to the activation of anabolic genes and repression of the catabolic genes through nucleosome-remodeling processes acting on differential chromatin structures. This results in the expression of the anabolic program, which leads to cellular growth. As ATP is consumed, the anabolic genes become down-regulated, the nucleosomes remodeling activity decreases, easing the repression of the catabolic genes. This leads to the expression of the catabolic program which results in increased ATP production. With the increasing ATP production, the mitochondria eventually becomes de-energized, halting energy production.

energy dependent general regulatory mechanism which underlies the global and pervasive expression dynamics.

A comparative analysis of two distinct oscillatory transcriptome datasets[31] reported that differentially expressed gene clusters have different nucleosome configurations in terms of positioning, occupancy and size of the NDR (nucleosome-depleted regions), and differential effects on nucleosome configurations of global transcription factor mutants and ATP-dependent nucleosome remodelers[43,44]. Chromatin remodeling in yeast is mediated by at least two complexes, RSC which is involved in maintaining nucleosome-free promoters for efficient transcription[45], and the Isw2 remodeling complex, which shifts nucleosomes towards the promoter regions to inhibit transcription[43] and appears to influence predominantly catabolic genes[31]. The activity of both these complexes is ATP dependent. These observations suggest chromatin structure as the target of ATP-driven regulation of transcription.

The proposed a dual negative feedback loop model (Fig. 2), that shapes gene expression to the energetic landscape, can have a highly oscillatory output. This involves ATP activation of the RSC complex resulting in the expression of genes with well defined nucleosome depleted regions, while simultaneously repressing the expression of catabolic genes through the Isw2 complex. Decreased intracellular ATP results in reversal of all these processes. Anabolism and catabolism become therefore globally partitioned: mediated by direct feedback loops between the energetic and redox state of the cell and chromatin state *via* enzymatic cofactors and coenzymes. This model is supported in higher eukaryotes by previously reported *in vivo* and *in vitro* ultradian oscillations in the nucleosome remodeling in glucocorticoid and estrogen systems, where pulses of stimulant or ATP caused a damped ultradian oscillation in nucleosome structure[46,47].

Recently, the respiratory oscillation has been correlated with the growth and the general stress responses of yeast [30,31]. The model proposed here can describe these phenomena with respect to ATP availability and chromatin remodeling, and would require only minimal regulation framework to switch cellular states, i.e., cells would express "growth" or "stress" expression profiles based on cellular energetics feeding back onto chromatin structure, through remodeling complexes.

Chapter 3 Quantifying periodicity in time-series, high-throughput datasets

Cellular network dynamics are excitable and inherently non-linear, properties that stem from the multitude of feedback and feedforward loops involved in biological processes[18,48]. These systems form an intimate feedback with the environment to generate the dynamic phenotype of the cell (e.g., oscillation/pulsing, bursting bistability)[49,50]. The feedback and feedforward systems have drastically different time scales that vary over several orders of magnitude[51] and the interaction between different dynamical processes remains poorly characterized. Understanding the dynamical interactions between time scales are key to understanding the complex phenotypes of embryogenesis[52], circadian biology in disease[53] and psychology[13,14].

Generally, analysis methods are restricted to the period of interest, such as the perturbation length or oscillation period, and the sampling frequency limits the use of many powerful time-series

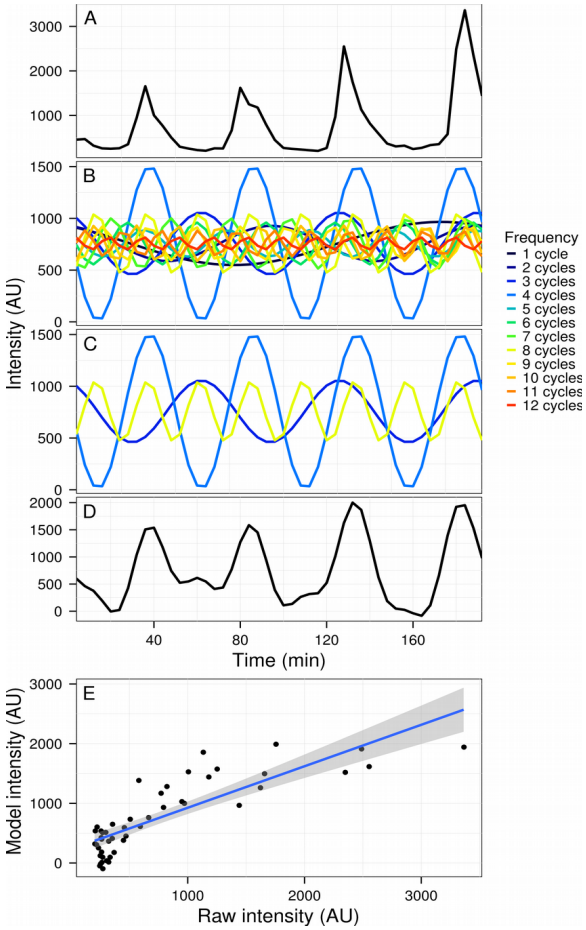

Figure 3 Graphical representation of the waveform model construction

The raw gene expression time-series of gene YAL067C (A; arbitrary fluorescence units) is first decomposed by fast Fourier transform (B). The significant powers which comprise the signal based on the significance cutoff specified (C) are then recomposed to produce the model (D). A linear fit is then used to determine the coefficient of variation (E; $R^2 = 0.695$) for the data (A) vs. the model (D).

analysis tools[54]. Autocorrelation[55] and Fourier transform[55,56] methods rely on targeting a particular frequency, and can be prone to generating false calls due to frequency changes and multi-oscillators. Singular Value Decomposition (SVD)/Principal Component Analysis (PCA) generally assumes that the largest variances are the most interesting (neglecting subtle effects), and also does not allow for the use of a priori knowledge to the analyses[57]. Furthermore, it is difficult to assign meaning to the contributions of each time-series to the components[58,59]. Wavelets analyses are powerful, but require data of higher density than high-throughput experiments usually provide[23,60–62]. Among the methods proposed, one major limitation is the inability to separate, quantify and unambiguously describe different periods in a multi-oscillatory signal. We[63] therefore focused on the discrete Fourier transform (DFT) spectral analysis, which addresses these issues, and developed a tool that expands on the signal-to-noise (SN) ratio approach[31,55]. After a DFT decomposition Fig. 3), the SN ratio and its significance for each frequency is calculated, the non significant frequencies are removed and the signal reconstructed, thus generating a model waveform, whose goodness of fit to the original data is calculated using the coefficient of determination (R^2) . The reasoning behind the construction of the model is that removing time-points for reducing the complexity of the dataset or smoothing time-series offers little control over

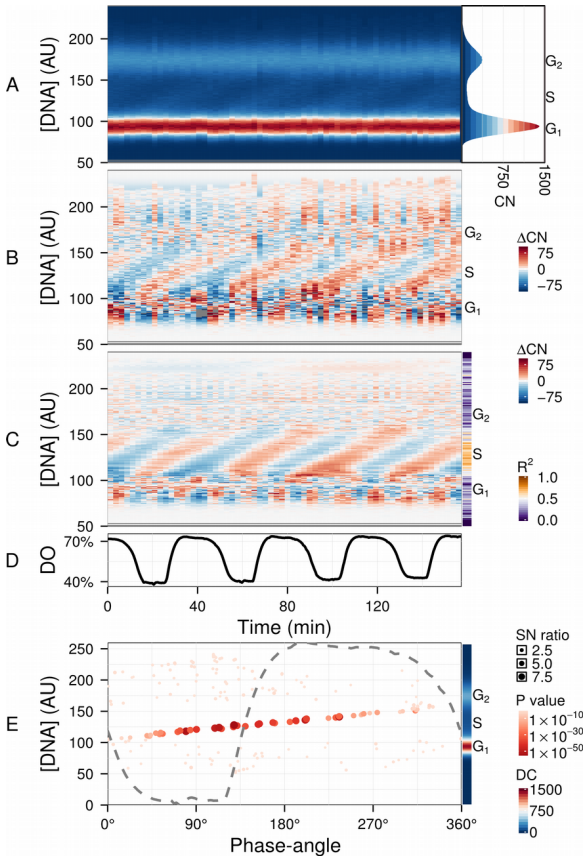

Figure 4 Identification of phase-relationships in a flow cytometry dataset[23]

Each datapoint represents the number of cells (CN) in a DNA intensity bin (peak propidium iodide channel)[20]. These were aligned and scaled according to the G_1 and G_2 peaks (A; histogram of the average CN over the time-series is shown in right panel). Residuals (B) were calculated by subtracting the average CN over the time-series and then filtered using the waveform algorithm (C; R^2 values in sidebar). The dissolved oxygen (DO) trace during the experiment is shown in D. The major component (4 cycles) was characterized by the phase-angles with respect to the respiratory oscillation and SN ratio at each DNA concentration (E); the mean (DC) is shown in sidebar. The dashed line represents the DO trace over one cycle, scaled to the range of the panel. Phase-angles 0°/360° indicate the phase of minimum DO uptake rate.

the temporal patterns that are being eliminated. However, a DFT decomposition of the dataset provides the user with means to decide which frequencies are of interest and remove low amplitude components or frequencies that are outside the temporal window analyzed.

The algorithm was developed in R[64] and is called `waveform`. The main parameters passed are the cutoff method (SN ratio or its P value) and cutoff threshold (default to 2 and 0.05, respectively). It can be used in an exploratory manner (untargeted approach, preserves all significant oscillatory components) or directed towards a set of periodicities (targeted approach, also screens out oscillatory components that are not targeted). The significance can be calculated using either a model or permutations. The statistics necessary for a full characterization of the Fourier components (DC, amplitude and phase) are also calculated.

The tool was used for clarifying the phase relationship, significance of oscillation and duration of the DNA division cycle in a flow cytometry time-series dataset[23] (Fig. 4A). While subtracting the background (Fig. 4B) already reveals the main patterns, information such as the precise timing of DNA replication with respect to the respiratory oscillation and the amplitude in the S-phase regions are not trivial to extract. The waveform model was used to accentuate the regions of interest by using an untargeted approach with the default parameters (Fig. 4C). Interestingly, S-phase was shown to be a linear time-series that continues throughout the respiratory cycle, starting during the phase where DO was lowest (Fig. 4E), which was earlier than previously reported[20], and may resolve conflicting timings of mid S-phase found for different oscillation periods[22,65]. This could only be observed after filtering out the contaminating frequency components from the much larger G_1 and G_2 cell cycle phase peaks.

The algorithm has a variety of other applications, such as exploratory analysis of mass spectrometry data, identification of differential responses to perturbation, and identification of least oscillatory values to assist normalization of highly oscillatory datasets[56,66]. The temporal characterization shown in Figure 4E, i.e., calculation of mean value (DC), phase-angle, SN ratio and its significance for a particular periodicity, provides metrics by which data across experiments can be easily correlated.

Chapter 4 Global DNA occupancy during the yeast respiratory cycle

The chromatin landscape, defined by the occupancy and the state of histone octamers along the DNA (nucleosomes), is a major determinant of gene transcription. While nucleosome positioning is partially determined by the DNA sequence[67–69], energy-dependent processes such as nucleosome remodeling[43,70,71]. The nucleosome downstream of TSS and the upstream nucleosome depleted region (NDR) stand out as a target of regulation for nucleosome remodeling complexes, where inclusion of the H2A.Z histone variant, covalent histone modifications and transcription factors facilitate the entry of RNA polymerase II (PolII) into the gene[71–74].

Previous studies have produced high-resolution maps of nucleosome positioning[69,75] and investigated genome-wide chromatin remodeling and histone modifications using chemical and/or genetic perturbations[44,71,76,77]. However, these studies rarely account or measure the energetic state of the culture, which is one of the principal drivers of chromatin remodeling, transcription and cellular growth. This is probably best exemplified by the strict requirement of ATP, but not of transcription or replication, for *in vitro* reconstitution of nucleosome configurations at promoters[70].

This study measured the genome-wide DNA occupancy using tiling arrays that were hybridized with DNA extracted from time-series samples taken over three respiratory cycles (Fig. 5). Spatially, the average DNA occupancy profiles around the transcription start sites of protein-coding genes (TSS; Fig. 5A) follow the canonical pattern of a NDR centered at ~75 bp upstream of TSS, flanked by well organized nucleosome arrays. Temporally, a DFT analysis of the dataset revealed the major period (67 minutes; 15% of probes; P value < 0.05), but it was immediately apparent that the DNA occupancy data comprises of higher frequencies (Fig. 5A). However, the resolution of the tiling arrays used made identification of nucleosomes unreliable, and a published high-resolution map of *S. cerevisiae* nucleosomal dyads[69] was cross-referenced with the DNA occupancy dataset to define preferential nucleosomal positions.

Nucleosomes found +2 to the penultimate nucleosome were defined as gene body nucleosomes (Fig. 5B; GB) and showed two peaks

per cycle ($GB_{60°}$ and $GB_{225°}$), while all nucleosomes found in NDR-flanking regions at both 5' and 3' ends of genes, including the TSS-covering nucleosome, show three peaks (Fig. 5B; $TSS_{75°}$, $TSS_{225°}$ and $TSS_{330°}$). $TSS_{225°}$ and the major $GB_{225°}$ events coincide, whereas $TSS_{75°}$ and $TSS_{330°}$ coincide with the metabolic transitions between oxidative and reductive phases. DNA occupancy at the NDR is lowest during two temporal windows (45° & 240°; Fig. 5A). To explore DNA occupancy data in the context of gene expression, the dataset was compared with the temporal program of co-expressed and functionally coherent gene cohorts during the respiratory oscillation[31]. Surprisingly, little difference could be observed in the temporal profiles of DNA occupancy at nucleosomal positions of the anabolic and catabolic clusters (Fig. 6A), despite differential transcription. Thus, a global chromatin restructuring event during the respiratory cycle occurs similarly for all genes regardless of promoter architecture.

To further characterize these genome-wide events in promoter, histone H3 presence and the

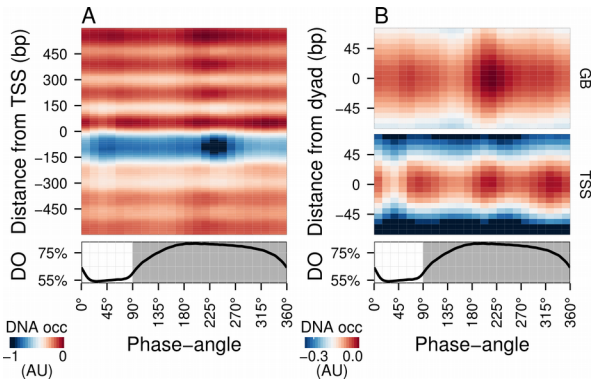

Figure 5 Average DNA occupancy dynamics around gene TSS per respiratory cycle

An average cycle was constructed by a cubic spline fitting of the dataset (normalized by the least variant set[66]) comprising three respiratory cycles (33 samples; sampling every 6 minutes; oscillation period 67 minutes), where protein-bound and genomic DNA sample pairs were extracted using a novel one-pot method. The average occupancy dynamics are shown as median DNA occupancy (color-coded, capped at –1 for increased resolution) around the TSS of 5140 genes (A) and around nucleosome dyads[69] (B), which were classified according to their position with respect to TSS: GB (gene body nucleosomes except for +1/terminal nucleosomes), TSS (nucleosome at TSS). Time is represented as phase-angles calculated according to the DO (represented as a subscript throughout the text), where the minimum first derivative of the DO data (bottom panels) represents 0°/360° and gray areas indicate the reductive phase.

acetylation state (H3K9ac:H3) were tested by ChIP-qPCR. Again, the differences between differentially transcribed genes are at best subtle, but show clear correlations to the global occupancy dynamics (Fig. 6A–C). TSS H3 occupancy gradually increases over the reductive phase in all genes and its peak coincides with the global event ($GB_{225°}$ & $TSS_{225°}$), not exhibiting major secondary peaks. In contrast, H3K9 acetylation is enriched at the two transition events that are seen at TSS, suggesting these peaks in TSS protein occupancy may rather reflect binding of promoter-remodeling or transcription initiation complexes rather than an increase histone occupancy. Notably, a large decrease in acetylation during the mid reductive phase coincides with the nucleosomal focusing event, providing evidence that this event was a result of histone deacetylation. The total transcript levels of the two superclusters (∑[mRNA]; Fig. 6D) were used to calculate global changes in transcript turnover (first derivative ∑[mRNA]'; Fig. 6E), which revealed a short increase, then sharp drop of ∑[mRNA]' in both superclusters at the nucleosomal focusing point, thus potentially reflecting a co-release of transcripts with PolII and a subsequent global halt on transcription, or increased RNA degradation. These transcription rate profiles closely matched the PolII occupancy in the gene body at two anabolic and two catabolic genes (Fig. 6F), confirming these changes are a result of transcriptional activity.

In summary, this study correlates DNA occupancy dynamics, mRNA expression timing and the metabolic state of the culture. Protein occupancy at NDR-flanking nucleosomes increases at the transitions between high and low energy states, coinciding with the transitions between the expression superclusters. A rapid sequence of genome-wide events occur after energy state has reached a minimum during the reductive phase, i.e., a genome-wide increase of histone occupancy, clearance of the NDR, and a global decrease in transcription rates. After this sequence, ATP:ADP recovers quickly and the expression of anabolic supercluster genes proceeds. These time-resolved data imply the observed nucleosome focusing event as a key step that resets transcription during the respiratory oscillation. Furthermore, while the three TSS events correspond to increases in transcript abundance globally, they are not reflected in the differential expression profiles of the anabolic and catabolic superclusters, suggesting that differential expression does not result from targeted chromatin remodeling, but stems from effects these global remodeling events

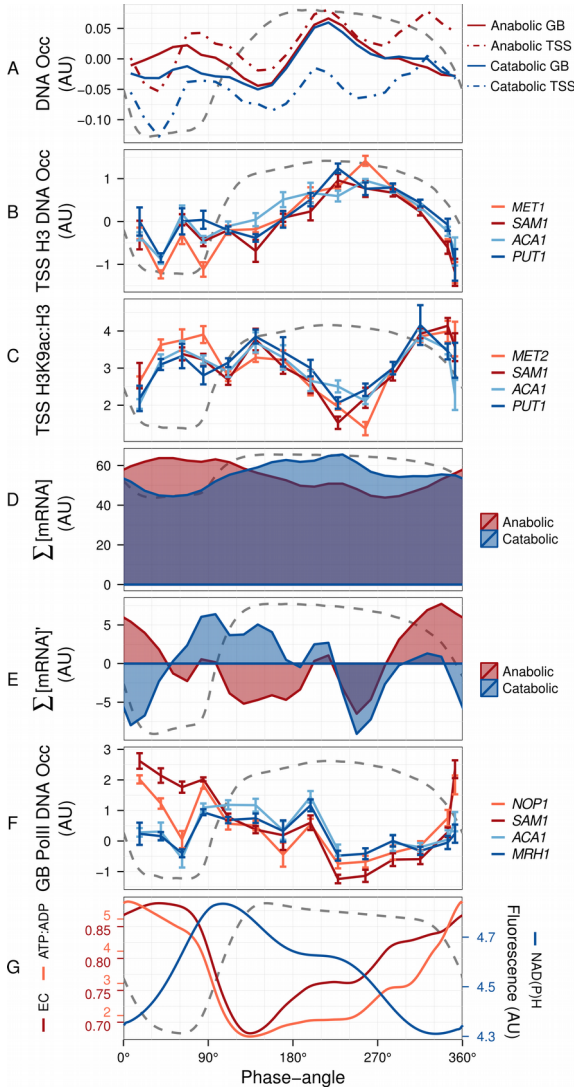

Figure 6 Defining the respiratory oscillation reset point

Median profiles aligned to gene nucleosome dyads of the anabolic and catabolic superclusters (A) were calculated as in Figure 5B. Histone H3 (B) and H3K9ac (C, log-ratio values with respect to H3) ChIP time-series (14 samples; sampled every 4 minutes; oscillation period 53 minutes) were amplified by qPCR at TSS regions of 2 anabolic (red hues) and 2 catabolic genes (blue hues). Total mRNA abundances[34] for each supercluster (D; ∑[mRNA]) were used to calculate mRNA abundance rate of change (E; ∑[mRNA]'), as the change in mRNA abundance every 15°. The same samples for B & C were used for PolII ChIP-qPCR at gene body of 2 anabolic (red hues) and 2 catabolic (blue hues) genes (F). PolII signals were normalized with respect to a subtelomeric region on chromosome VI. ATP:ADP and EC (G, red hues) were calculated from CE-MS measured ADP & ATP concentrations[40] . NAD(P)H (G, blue) was measured by *in situ* fluorimetry[32]. An average cycle was constructed by a cubic spline fitting for each time-series spanning several cycles (A, D, E, G). Error bars in B, C, F represent the standard error of mean of qPCR triplicates. Dotted lines represent the DO, scaled to the y-axis range, and datasets were aligned using the minimum and maximum first derivative of DO. The minimum first derivative of the DO data represents 0°/360°.

have on different promoter structures.

Chapter 5 The influence of intergenic distances on gene expression

Upstream nucleosomes (namely –1, –2) are commonly thought to regulate the exposure of the promoter and the recruitment of factors necessary for transcription, and are often represented in the regulatory structure of the gene. By extension, the length of the nucleosome depleted region (NDR) which is formed between the +1 and –1 nucleosomes, is considered a crucial factor in transcription regulatory processes such as the incorporation of the H2A.Z histone variant and the recruitment of nucleosome remodeling complexes[73,74]. However, when taking into consideration the compactness of the yeast genome where intergenic regions, calculated from start to start/end codons are on average shorter than 400 bp and can be as short as 71 bp[78], it is soon apparent that many upstream nucleosomes intersect with the upstream features (e.g., other genes). Recent nucleosome maps revealed that few well-positioned nucleosomes can be seen outside non-coding regions[70,75], and that nucleosome in intergenic regions have shorter inter-dyad distances, thus are sometimes partially wrapped[79].

Analysis of the distance from gene TSS to the start/end of adjacent upstream features showed that a majority of genes are less than 305 bp away from their neighbor (distance referred to as the length of the upstream regulatory region, URR). Since most start and end codons are occluded by a well-position nucleosome, this distance is comparable to the length of the NDR if no well-positioned nucleosomes were to be found in this intergenic region. Indeed, the distribution of the URR peaks at 225 bp, which coincides with position of the –1 nucleosome on a majority of genes (200 – 250 bp upstream of TSS)[80], suggesting that –1 nucleosomes are often the well-positioned +1 or terminal nucleosomes of the upstream feature, and that the upstream NDR length is mostly dictated by this intergenic distance. Moreover, the URR length distribution did not show any secondary peaks, suggesting the URR length, and by extension the NDR length, do not occur at any set frequency overall. This confirms recent data[81] which shows a continuum of positions where the –1 nucleosome could be found. When taking the directionality of the intergenic regions into account, the divergent regions (where two gene promoters are shared or

adjacent) have an apparent ~200 bp periodicity, while unidirectional regions (where the promoter of a gene is adjacent to the end of another gene) did not have visible periodicities.

The URR length was binned to the average distance between dyads (~162bp[69]) and promoter structure averages (Fig. 7A) confirmed that, in a

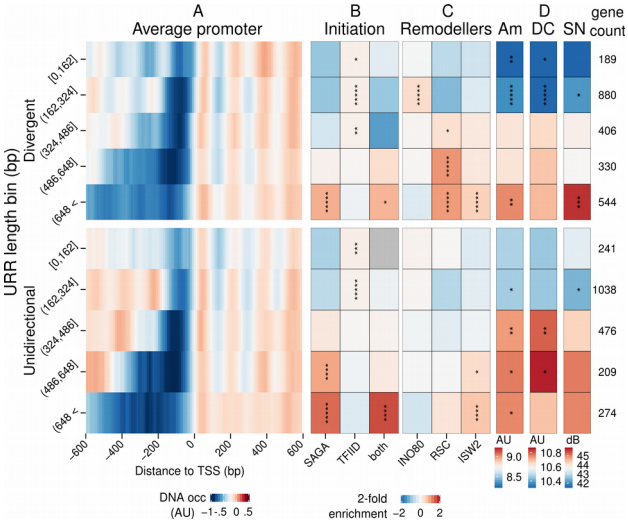

Figure 7 Promoter structure, transcription initiation machinery, remodeling activity and gene expression statistics with respect to intergenic (URR) length

The distance from TSS to the nearest upstream start or stop codon (x-axis) of 3816 genes (excluding genes with unknown TSS, their upstream and non-protein coding features) was binned by 162 bp and classified by the directionality of adjacent genes (divergent = opposite strands, unidirectional = same strand). The number of genes in each bin is shown in the rightmost column. A static promoter profile for each gene group (A) was obtained by averaging all time-points of the DNA occupancy dataset (Fig. 1A). The enrichment of genes classified by their dominant transcriptional machinery[82] (B), and binding targets (C) of INO80[84], RSC[83] and Isw2[43] were calculated by hypergeometric tests, and the color gradients for B and C indicate 2-fold enrichment compared to the expected number of hits assuming a normal distribution; gray indicates 0 hits. Statistics on gene expression (D), namely the amplitude of the transcriptional oscillation (Am, log2), mean expression (DC, log2) and signal-to-noise ratio (SNR, decibels) for each gene were obtained using a DFT decomposition (Fig. 4D) on a time-series expression dataset[34]. White denotes the mean value for each statistic in the dataset, and P values were calculated by t-test. In all panels, *: P value < 0.05, **: P value < 0.005, ***: P value < 0.0005, ****: P value < 0.00005.

majority of genes, the first upstream nucleosome coincides with the start of the upstream feature (in the divergent case) or the end of the upstream feature (in the unidirectional case), thus supporting the equivalence of the URR and the upstream NDR. Moreover, when the dominant transcription initiation machinery[82] was compared to the URR length (Fig. 7B), the TFIID-dominated genes (representing ~80% of genes) are enriched in short URR genes in both divergent and unidirectional gene pairs, and SAGA-dominated targets are enriched in genes with longer unidirectional URR or very long URR.

The URR of the gene targeted by various chromatin remodelers[43,83,84] (Fig. 7C) was analyzed, and it was apparent that remodelers investigated are principally enriched in divergent genes. A high enrichment of INO80 targets was primarily found on shorter URR, which agrees with the more regular nucleosomal distributions that can be observed on these genes[85,86]. Divergent genes spaced further apart are enriched in RSC targets, while unidirectional gene pairs show little significant enrichment of chromatin remodelers by URR length, except for the very long URR genes that are enriched in Isw2 remodeling regardless of directionality. This indicates an increased regulation on genes that share promoters. The URR length also showed a significant positive correlation with the expression mean, amplitude, and signal-to-noise ratio[34] (Fig. 7D).

Adjacent divergent gene pairs in high proximity show strong temporal correlations in both superclusters, suggesting that their transcription is initiated simultaneously. The noisy expression clusters, which encompass a third of the yeast genome and generally have short URR, are most enriched in this co-expression, reflecting the overall trend of the transcriptional program which starts at high energy levels and stops when chromatin structure is reset (Fig. 5). The high correlation with ATP dynamics (Fig. 1C) suggests these genes are not under specific regulatory mechanisms, but are most influenced by cofactor availability, hindered by the small NDR, resulting in a low abundance, "noisy" expression.

In summary, a majority of genes either do not have upstream nucleosomes or share their single upstream nucleosome with the adjacent feature, thus questioning the regulatory importance of these nucleosomes. The intergenic distance between adjacent features showed a positive correlation with gene expression levels, signal-to-noise and amplitude, and a negative correlation with the well-positioning of nucleosomes and nucleosome occupancy levels observed in the gene body, suggesting these properties could be a side-effect of the nucleosomal crowding on the genome. These results did not translate in differences between anabolic and catabolic genes, but provided substantial clues on the temporal

organization of divergent pairs of genes which tend to be co-expressed (that likely share promoters or have adjacent promoters). Further studies should focus on the DNA structure, e.g., the positioning of TATA boxes with respect to nucleosomes and common DNA sequences[31], and the potential mechanisms of co-regulation of adjacent or overlapping promoters.

Chapter 6 Concluding remarks

Rhythmicity plays a significant role in biological systems, with examples spanning a wide range of time-scale domains, from milliseconds to hundreds of years, and careful orchestration of these time-scales is required in order to maintain spatio-temporal coherence from cells to ecosystems. Cellular rhythms in particular are being investigated with increasing interest due to evidence that their interplay with circadian rhythmicity has significant health implications. However, technical limitations in acquiring high-density time-series samples that are either synchronized with respect to the rhythm being investigated or monitoring single cells without perturbation present a bottleneck for these investigations. Yeast continuous cultures, in which individual cells auto-synchronize their behavior to produce stable ultradian respiratory oscillations that can be precisely monitored provide an ideal system for studying cellular dynamics.

The yeast respiratory oscillation has clock characteristics and displays an alternation of oxidative and reductive cellular states. Previous high-throughput time-series analyses showed that transcription, metabolite production and DNA replication are highly oscillatory and have a phase-relationship with the respiratory cycle. Computational analyses revealed a temporal separation between the anabolic and catabolic transcriptional programs which occur out-of-phase with the physiology, where the "switch" points correlated with changes in energetic and redox states. Comparisons between these differentially-expressed gene cohorts and a compendium of high-throughput datasets available for yeast genes pointed to chromatin structure and remodeling as the discriminating factor. Taken together, these data led to a model of gene transcription regulation in which cellular energetics feedback on the chromatin state through nucleosome remodeling or nucleosome modifications, resulting in differential transcription of the anabolic and catabolic cohorts depending on energy availability.

To address issues related to characterizing and correlating periodicity in the increasing amount of high-throughput time-series data on the physiology, cell cycle, redox biochemistry, energetics, metabolism, transcription, post-translational modifications, etc., computational tools to identify and quantify multi-periodicities were developed. These tools can be used for processing, normalizing, clustering data and identifying biological signals without distorting the temporal structure of the dataset.

Following the evidence that points to a global regulation of chromatin structure through energy-dependent processes, the DNA occupancy was investigated during the respiratory cycle, for which time-series friendly protein-bound DNA extraction methods were also developed. The study revealed a point of global nucleosome focusing that temporally coincides with a general transcriptional slow-down, between the end of the catabolic and beginning of the anabolic supercluster transcription. Evidence indicates this event is facilitated by global histone deacetylation, and the subsequent global acetylation event kick-starts the transcription of the anabolic supercluster. This chromatin reset point provides a mechanistic explanation for the shut-down of catabolism when energy becomes available and the subsequent start of the anabolic program.

When put in the context of circadian rhythms, where a similar succession of events has been observed[87], the existence of this reset point, that corresponds to a point of high robustness to oxidative stress in the yeast continuous culture system[88], may explain the resilience of pathogens and tumors, considering the cell heterogeneity. Furthermore, evidence that tumor cell growth is coupled with circadian rhythmicity of the host[89,90], but that the temporal windows in which the host and tumor cells undergo DNA replication may be out of phase with each other[91] imply that the efficiency of chemotherapy could be greatly enhanced by taking into account the timing of drug delivery.

Another significant result of this study was that RNA polymerase II occupancy, nucleosome occupancy and acetylation levels display global oscillatory patterns that are not dictated by the gene transcription timing, but instead seem to be determined by the cellular state. This supports the hypothesis that differential regulation of

transcription is encoded in the gene promoter structure, providing a substrate that responds differently to the same cellular environment. A computational analysis of the nucleosomal landscape at gene promoters found that, due to the compactness of the yeast genome, a majority of genes either do not have upstream nucleosomes or share their single upstream nucleosome with the adjacent feature, thus questioning the regulatory importance of these upstream nucleosomes. Furthermore, the intergenic distance between adjacent features showed a positive correlation with gene expression levels, signal-to-noise and amplitude, and a negative correlation with the well-positioning of nucleosomes and nucleosome occupancy levels observed in the gene body, suggesting these properties could be a side-effect of the nucleosomal crowding on the genome. The predominant initiation machinery was also found to be differentially enriched in genes with long and short upstream intergenic distances. These results did not translate in differences between anabolic and catabolic genes, but provided substantial clues on the temporal organization of divergent pairs of genes (that are likely sharing their promoter region or have adjacent promoters), which tend to be co-expressed. Overall, these studies emphasize the importance of the chromatin structure at promoter regions, but put in question the regulatory role of nucleosomes found outside gene bodies, and instead suggest further studies should be undertaken on the DNA structure, such as the positioning of TATA boxes with respect to nucleosomal dyads and common DNA sequences[31], the spacing between genomic features, and the potential mechanisms of co-regulation of adjacent or overlapping promoters.

Taken together, the results presented indicate global chromatin dynamics, that are largely driven by the cellular energetic and redox state. The regulation of anabolic and catabolic gene expression programs is likely carried out through differential effects of chromatin remodeling complexes acting on differential DNA structure of promoter region. Considering the observed drop in nucleosome occupancy specific only to TSS nucleosomes, which occurs at the transition between the anabolic and catabolic transcriptional programs, this regulation may only affect these nucleosomes, where shifts of less than 10 bp can hinder transcription[43,71]. Therefore, obtaining time-series data in which the metabolic state is taken into account to assess the activity of chromatin remodeling complexes at these regions is crucial for uncovering the precise mechanisms of gene regulation.

List of references

1. Chrobak, J. J. & Buzsáki, G. Gamma oscillations in the entorhinal cortex of the freely behaving rat. J Neurosci 18, 388–98 (1998).
2. Janzen, D. H. Why Bamboos Wait so Long to Flower. Annu Rev Ecol Syst 7, 347–91 (1976).
3. Gillette, M. U. & Sejnowski, T. J. Physiology. Biological clocks coordinately keep life on time. Science 309, 1196–8 (2005).
4. Lloyd, D. & Murray, D. B. Ultradian metronome: timekeeper for orchestration of cellular coherence. Trends Biochem Sci 30, 373–7 (2005).
5. Moser, M., Frühwirth, M. & Kenner, T. The symphony of life. Importance, interaction, and visualization of biological rhythms. IEEE Eng Med Biol Mag 27, 29–37 (2008).
6. Aon, M. A. et al. The scale-free dynamics of eukaryotic cells. PLoS One 3, e3624 (2008).
7. Lloyd, D. & Murray, D. B. Redox rhythmicity: clocks at the core of temporal coherence. Bioessays 29, 465–73 (2007).
8. Haydon, M. J., Hearn, T. J., Bell, L. J., Hannah, M. A. & Webb, A. A. R. Metabolic regulation of circadian clocks. Semin Cell Dev Biol 24, 414–21 (2013).
9. Edgar, R. S. et al. Peroxiredoxins are conserved markers of circadian rhythms. Nature 485, 459–64 (2012).
10. Lowrey, P. L. & Takahashi, J. S. Mammalian circadian biology: elucidating genome-wide levels of temporal organization. Annu Rev Genomics Hum Genet 5, 407–41 (2004).
11. Wijnen, H. & Young, M. W. Interplay of circadian clocks and metabolic rhythms. Annu Rev Genet 40, 409–48 (2006).
12. Gallego, M. & Virshup, D. M. Post-translational modifications regulate the ticking of the circadian clock. Nat Rev Mol Cell Biol 8, 139–48 (2007).
13. Salomon, R. M. & Cowan, R. L. Oscillatory serotonin function in depression. Synapse 67, 801–20 (2013).
14. Salvatore, P., Indic, P., Murray, G. & Baldessarini, R. J. Biological rhythms and mood disorders. Dialogues Clin Neurosci 14, 369–79 (2012).
15. Turek, F. W. et al. Obesity and metabolic syndrome in circadian Clock mutant mice. Science 308, 1043–5 (2005).
16. Lie, J.-A. S., Roessink, J. & Kjaerheim, K. Breast cancer and night work among Norwegian nurses. Cancer Causes Control 17, 39–44 (2006).
17. Videnovic, A. & Golombek, D. Circadian and sleep disorders in Parkinson's disease. Exp Neurol 243, 45–56 (2013).
18. Lloyd, D. in Ultradian Rhythms from Molecules to Mind (eds. Lloyd, D. & Rossi, E. L.) 5–22 (Springer Netherlands, 2008).
19. Lloyd, D., Edwards, S. W., Williams, J. L. & Evans, B. J. Mitochondrial cytochromes of *Acanthamoeba castellanii*: Oscillatory accumulation of haemoproteins, immunological determinants and activity during the cell cycle. FEMS Microbiol Lett 16, 307–12 (1983).
20. Klevecz, R. R., Bolen, J., Forrest, G. & Murray, D. B. A genomewide oscillation in transcription gates DNA replication and cell cycle. Proc Natl Acad Sci U S A 101, 1200–5 (2004).
21. Murray, D. B., Beckmann, M. & Kitano, H. Regulation of yeast oscillatory dynamics. Proc Natl Acad Sci U S A 104, 2241–6 (2007).
22. Slavov, N., Macinskas, J., Caudy, A. & Botstein, D. Metabolic cycling without cell division cycling in respiring yeast. Proc Natl Acad Sci U S A 108, 19090–5 (2011).
23. Sasidharan, K., Tomita, M., Aon, M., Lloyd, D. & Murray, D. B. Time-structure of the yeast metabolism in vivo. Adv Exp Med Biol 736, 359–79 (2012).
24. Silverman, S. J. et al. Metabolic cycling in single yeast cells from unsynchronized steady-state populations limited on glucose or phosphate. Proc Natl Acad Sci U S A 107, 6946–51 (2010).
25. Jacquet, M., Renault, G., Lallet, S., De Mey, J. & Goldbeter, A. Oscillatory nucleocytoplasmic shuttling of the general stress response transcriptional activators Msn2 and Msn4 in *Saccharomyces cerevisiae*. J Cell Biol 161, 497–505 (2003).
26. Shedden, K. Analysis of cell-cycle gene expression in *Saccharomyces cerevisiae* using microarrays and multiple synchronization methods. Nucleic Acids Res 30, 2920–9 (2002).
27. Finn, R. K. & Wilson, R. E. Fermentation Process Control, Population Dynamics of a Continuous Propagator for Microorganisms. J Agric Food Chem 2, 66–9 (1954).
28. Von Meyenburg, H. K. Energetics of the budding cycle of *Saccharomyces cerevisiae* during glucose limited aerobic growth. Arch Mikrobiol 66, 289–303 (1969).
29. Murray, D. B. The respiratory oscillation in yeast phase definitions and periodicity. Nat Rev Mol Cell Biol 7, (2006).

30. Slavov, N. & Botstein, D. Coupling among growth rate response, metabolic cycle, and cell division cycle in yeast. Mol Biol Cell 22, 1997–2009 (2011).
31. Machné, R. & Murray, D. B. The yin and yang of yeast transcription: elements of a global feedback system between metabolism and chromatin. PLoS One 7, e37906 (2012).
32. Murray, D. B., Engelen, F., Lloyd, D. & Kuriyama, H. Involvement of glutathione in the regulation of respiratory oscillation during a continuous culture of *Saccharomyces cerevisiae*. Microbiology 145, 2739–45 (1999).
33. Tu, B. P., Kudlicki, A., Rowicka, M. & McKnight, S. L. Logic of the yeast metabolic cycle: temporal compartmentalization of cellular processes. Science 310, 1152–8 (2005).
34. Li, C. M. & Klevecz, R. R. A rapid genome-scale response of the transcriptional oscillator to perturbation reveals a period-doubling path to phenotypic change. Proc Natl Acad Sci U S A 103, 16254–9 (2006).
35. Murray, D. B., Roller, S., Kuriyama, H. & Lloyd, D. Clock control of ultradian respiratory oscillation found during yeast continuous culture. J Bacteriol 183, 7253–9 (2001).
36. Matsuo, T. et al. Control mechanism of the circadian clock for timing of cell division in vivo. Science 302, 255–9 (2003).
37. Xu, Z. & Tsurugi, K. A potential mechanism of energy-metabolism oscillation in an aerobic chemostat culture of the yeast *Saccharomyces cerevisiae*. FEBS J 273, 1696–709 (2006).
38. Liu, Y. et al. Circadian orchestration of gene expression in cyanobacteria. Genes Dev 9, 1469–78 (1995).
39. Minami, Y. et al. Measurement of internal body time by blood metabolomics. Proc Natl Acad Sci U S A 106, 9890–5 (2009).
40. Sasidharan, K., Soga, T., Tomita, M. & Murray, D. B. A yeast metabolite extraction protocol optimised for time-series analyses. PLoS One 7, e44283 (2012).
41. Rey, G. & Reddy, A. B. Connecting cellular metabolism to circadian clocks. Trends Cell Biol 23, 234–41 (2013).
42. Ball, W. J. & Atkinson, D. E. Adenylate energy charge in *Saccharomyces cerevisiae* during starvation. J Bacteriol 121, 975–82 (1975).
43. Whitehouse, I., Rando, O. J., Delrow, J. & Tsukiyama, T. Chromatin remodelling at promoters suppresses antisense transcription. Nature 450, 1031–5 (2007).
44. Badis, G. et al. A library of yeast transcription factor motifs reveals a widespread function for Rsc3 in targeting nucleosome exclusion at promoters. Mol Cell 32, 878–87 (2008).
45. Fischer, C. J., Saha, A. & Cairns, B. R. Kinetic model for the ATP-dependent translocation of *Saccharomyces cerevisiae* RSC along double-stranded DNA. Biochemistry 46, 12416–26 (2007).
46. Métivier, R. et al. Estrogen receptor-alpha directs ordered, cyclical, and combinatorial recruitment of cofactors on a natural target promoter. Cell 115, 751–63 (2003).
47. Nagaich, A. K., Walker, D. A., Wolford, R. & Hager, G. L. Rapid periodic binding and displacement of the glucocorticoid receptor during chromatin remodeling. Mol Cell 14, 163–74 (2004).
48. Novák, B. & Tyson, J. J. Design principles of biochemical oscillators. Nat Rev Mol Cell Biol 9, 981–91 (2008).
49. Sobie, E. A. Bistability in biochemical signaling models. Sci Signal 4, tr10 (2011).
50. Levine, J. H., Lin, Y. & Elowitz, M. B. Functional roles of pulsing in genetic circuits. Science 342, 1193–200 (2013).
51. Aon, M. A., Cortassa, S. & O'Rourke, B. Percolation and criticality in a mitochondrial network. Proc Natl Acad Sci U S A 101, 4447–52 (2004).
52. Kageyama, R., Niwa, Y., Isomura, A., González, A. & Harima, Y. Oscillatory gene expression and somitogenesis. Wiley Interdiscip Rev Dev Biol 1, 629–41 (2012).
53. Gibbison, B., Angelini, G. D. & Lightman, S. L. Dynamic output and control of the hypothalamic-pituitary-adrenal axis in critical illness and major surgery. Br J Anaesth 111, 347–60 (2013).
54. Dowse, H. B. Statistical analysis of biological rhythm data. Methods Mol Biol 362, 29–45 (2007).
55. Yamada, R. & Ueda, H. R. Microarrays: statistical methods for circadian rhythms. Methods Mol Biol 362, 245–64 (2007).
56. Lehmann, R. et al. How cyanobacteria pose new problems to old methods: challenges in microarray time series analysis. BMC Bioinformatics 14, 133 (2013).
57. Wang, D., Arapostathis, A., Wilke, C. O. & Markey, M. K. Principal-oscillation-pattern analysis of gene expression. PLoS One 7, e28805 (2012).
58. Raychaudhuri, S., Stuart, J. M. & Altman, R. B. Principal components analysis to summarize microarray experiments: application to sporulation time series. Pac Symp Biocomput 455–66 (2000).
59. Alter, O., Brown, P. O. & Botstein, D. Generalized singular value decomposition for comparative analysis of genome-scale expression data sets of two different organisms. Proc Natl Acad Sci U S A 100, 3351–6 (2003).
60. Klevecz, R. R. & Murray, D. B. Genome wide oscillations in expression. Wavelet analysis of time series data from yeast expression arrays uncovers the dynamic architecture of phenotype. Mol Biol Rep 28, 73–82 (2001).
61. Song, J. Z., Duan, K. M., Ware, T. & Surette, M. The wavelet-based cluster analysis for temporal gene expression data. EURASIP J Bioinform Syst Biol 2007, 39382 (2007).
62. Prasad, S. & Bruce, L. M. Limitations of Principal Components Analysis for Hyperspectral Target Recognition. IEEE Geosci Remote Sens Lett 5, 625–9 (2008).
63. Amariei, C., Tomita, M. & Murray, D. B. Quantifying periodicity in omics data. Front Cell Dev Biol 2, (2014).
64. R Development Core Team. R: A Language and Environment for Statistical Computing. (2008). at <http://www.r-project.org>
65. Amariei, C. et al. The dynamics of cellular energetics during continuous yeast culture. Conf Proc Annu Int Conf IEEE Eng Med Biol Soc 2013, 2708–11 (2013).
66. Calza, S., Valentini, D. & Pawitan, Y. Normalization of oligonucleotide arrays based on the least-variant set of genes. BMC Bioinformatics 9, 140 (2008).
67. Flores, O. & Orozco, M. nucleR: a package for non-parametric nucleosome positioning. Bioinformatics 27, 2149–50 (2011).
68. Suter, B. Poly(dAmiddle dotdT) sequences exist as rigid DNA structures in nucleosome-free yeast promoters in vivo. Nucleic Acids Res 28, 4083–9 (2000).
69. Brogaard, K., Xi, L., Wang, J.-P. & Widom, J. A map of nucleosome positions in yeast at base-pair resolution. Nature 486, 496–501 (2012).
70. Zhang, Z. et al. A packing mechanism for nucleosome organization reconstituted across a eukaryotic genome. Science 332, 977–80 (2011).
71. Van Bakel, H. et al. A compendium of nucleosome and transcript profiles reveals determinants of chromatin architecture and transcription. PLoS Genet 9, e1003479 (2013).
72. Albert, I. et al. Translational and rotational settings of H2A.Z nucleosomes across the *Saccharomyces cerevisiae* genome. Nature 446, 572–6 (2007).
73. Ranjan, A. et al. Nucleosome-free region dominates histone acetylation in targeting SWR1 to promoters for H2A.Z replacement. Cell 154, 1232–45 (2013).
74. Yen, K., Vinayachandran, V. & Pugh, B. F. SWR-C and INO80 chromatin remodelers recognize nucleosome-free regions near +1 nucleosomes. Cell 154, 1246–56 (2013).
75. Rhee, H. S. & Pugh, B. F. Genome-wide structure and organization of eukaryotic pre-initiation complexes. Nature 483, 295–301 (2012).
76. Lenstra, T. L. et al. The specificity and topology of chromatin interaction pathways in yeast. Mol Cell 42, 536–49 (2011).
77. Weiner, A. et al. Systematic dissection of roles for chromatin regulators in a yeast stress response. PLoS Biol 10, e1001369 (2012).
78. Chen, W.-H., Wei, W. & Lercher, M. J. Minimal regulatory spaces in yeast genomes. BMC Genomics 12, 320 (2011).
79. Chereji, R. V & Morozov, A. V. Ubiquitous nucleosome crowding in the yeast genome. Proc Natl Acad Sci U S A 111, 5236–41 (2014).
80. Lee, W. et al. A high-resolution atlas of nucleosome occupancy in yeast. Nat Genet 39, 1235–44 (2007).
81. Flores, O., Deniz, O., Soler-López, M. & Orozco, M. Fuzziness and noise in nucleosomal architecture. Nucleic Acids Res 42, 4934–46 (2014).
82. Huisinga, K. L. & Pugh, B. F. A Genome-Wide Housekeeping Role for TFIID and a Highly Regulated Stress-Related Role for SAGA in *Saccharomyces cerevisiae*. Mol Cell 13, 573–85 (2004).
83. Ng, H. H., Robert, F., Young, R. A. & Struhl, K. Genome-wide location and regulated recruitment of the RSC nucleosome-remodeling complex. Genes Dev 16, 806–19 (2002).
84. Yen, K., Vinayachandran, V., Batta, K., Koerber, R. T. & Pugh, B. F. Genome-wide nucleosome specificity and directionality of chromatin remodelers. Cell 149, 1461–73 (2012).
85. Udugama, M., Sabri, A. & Bartholomew, B. The INO80 ATP-dependent chromatin remodeling complex is a nucleosome spacing factor. Mol Cell Biol 31, 662–73 (2011).
86. Gkikopoulos, T. et al. A role for Snf2-related nucleosome-spacing enzymes in genome-wide nucleosome organization. Science 333, 1758–60 (2011).
87. Koike, N. et al. Transcriptional architecture and chromatin landscape of the core circadian clock in mammals. Science 338, 349–54 (2012).
88. Wang, J. et al. Cellular stress responses oscillate in synchronization with the ultradian oscillation of energy metabolism in the yeast *Saccharomyces cerevisiae*. FEMS Microbiol Lett 189, 9–13 (2000).
89. Filipski, E. Host Circadian Clock as a Control Point in Tumor Progression. CancerSpectrum Knowl Environ 94, 690–7 (2002).
90. Fu, L. & Kettner, N. M. The circadian clock in cancer development and therapy. Prog Mol Biol Transl Sci 119, 221–82 (2013).
91. Klevecz, R. R. & Braly, P. S. Circadian and Ultradian Cytokinetic Rhythms of Spontaneous Human Cancer. Ann N Y Acad Sci 618, 257–76 (1991).